Analyses of heterogeneous deformation and subsurface fatigue crack generation in alpha titanium alloy at low temperature

Osamu Umezawa, Motoaki Morita, Takayuki Yuasa, Satoshi Morooka, Yoshinori Ono, Tetsumi Yuri, and Toshio Ogata

Citation: AIP Conference Proceedings **1574**, 34 (2014); doi: 10.1063/1.4860601
View online: http://dx.doi.org/10.1063/1.4860601
View Table of Contents: http://scitation.aip.org/content/aip/proceeding/aipcp/1574?ver=pdfcov
Published by the AIP Publishing

Analyses of Heterogeneous Deformation and Subsurface Fatigue Crack Generation in Alpha Titanium Alloy at Low Temperature

Osamu Umezawa[a], Motoaki Morita[a*], Takayuki Yuasa[a †], Satoshi Morooka[a ¶], Yoshinori Ono[b], Tetsumi Yuri[b] and Toshio Ogata[b]

[a]*Department of Mechanical Engineering and Materials Science, Yokohama National University 79-5 Tokiwadai, Hodogaya, Yokohama, 240-8501, Japan*
[b]*National Institute for Materials Science, 1-2-1 Sengen, Tsukuba, 305-0047, Japan*
[*]*Now Tokyo University of Marine Science and Technology, Koto-ku, Tokyo 135-8533, Japan*
[†]*Now Nippon Steel & Sumitomo Metal, Kashima, 314-0014, Japan*
[¶]*Now Tokyo Metropolitan University, Hino, Tokyo 191-0065, Japan*

Abstract. Subsurface crack initiation in high-cycle fatigue has been detected as {0001} transgranular facet in titanium alloys at low temperature. The discussion on the subsurface crack generation was reviewed. Analyses by neutron diffraction and full constraints model under tension mode as well as crystallographic identification of the facet were focused. The accumulated tensile stress along <0001> may be responsible to initial microcracking on {0001} and the crack opening.

Keywords: fatigue, cracks, diffraction, strain incompatibility, Taylor factor, critical resolved shear stress, titanium
PACS: 62.20.mt

INTRODUCTION

Fatigue crack initiation is generally understood to occur on a specimen surface due to irreversible process of extrusion and intrusion thorough slip deformation. Subsurface fatigue crack generation of α-titanium alloys, however, is dominant in high-cycle regime and at lower temperature.[1-2] The subsurface crack initiation sites appear crystallographic a transgranular facet or facets. Dislocation movement of the alloys is fairly planar and dislocation arrays on {01-10}<11-20> are piled-up in the vicinity of grain boundaries.[1,3] The local stress concentration near a grain boundary due to the heterogeneous slip may cause the subsurface crack initiation and lower the high-cycle fatigue strength.

Here, the fatigue process is divided into four stages: 1) development of a saturated dislocation structure by cyclical micro-plastic strain accumulation, 2) generation of localized slip and/or microcracking to relax the stress concentration in the vicinity of a boundary, 3) microcrack growth and transition to main crack, and 4) crack propagation. In the stages 3) and 4), linear mechanics can be applied to evaluate the critical size of the subsurface crack (facet) for propagation [1,4] and the crack propagation life [5]. However, the stages 1) and 2), which are based on estimated models, do not exhibit direct evidence of cracking and macroscopic support. Thus, the evaluation based on crystal plasticity complements the construction of a sophisticated model of subsurface fatigue crack initiation. In the stage 1), the {01-10}<11-20> slip predominantly operates in some grains. The restriction of other slip systems results from their critical resolved shear stresses (CRSSs) as shown in Figure 1. Moreover, both plastic and elastic deformations coexist in polycrystalline specimens, since the operation depends on the crystal orientation. In the stage 2), regardless of whether the origin of transgranular cracking is slip-off (slip localization) [7] or microcracking [8] on a crystal plane, the plastic deformation on the facet plane hardly yields and the elastic field normal to the facet plane has to accumulate. Table 1 represents crystallographic characterization of the transgranular facet at subsurface crack initiation sites in the references [3,7,9-16]. The {0001} facet was commonly detected regardless of uniaxial loading mode as normal cyclic fatigue (normal), dwell cyclic fatigue (dwell) and static stress fatigue (static). Some traces of microcrack growth appeared on the facet, which may result from the slips on {0001}<11-20> and {01-10}<11-20>.[9] The longer the holding time at maximum cyclic stress was, the more the {01-10} step appeared on

Advances in Cryogenic Engineering
AIP Conf. Proc. 1574, 34-41 (2014); doi: 10.1063/1.4860601

the facet. The {01-10} facet was also reported under dwell fatigue test for highly textured alloy with <0001> perpendicular to tensile axis.[15]

These experimental analyses suggest that strain incompatibility due to heterogeneous deformation may form an opening stress along <0001> and generate crystallographic facet, but can hardly demonstrate cracking behavior itself. In the present review, the works on both neutron diffraction and Taylor analyses under tension mode were focused as well as the characterization of facet at the subsurface crack initiation site in order to discuss the influence of heterogeneous deformation on the transgranular cracking and its growth in α-titanium.

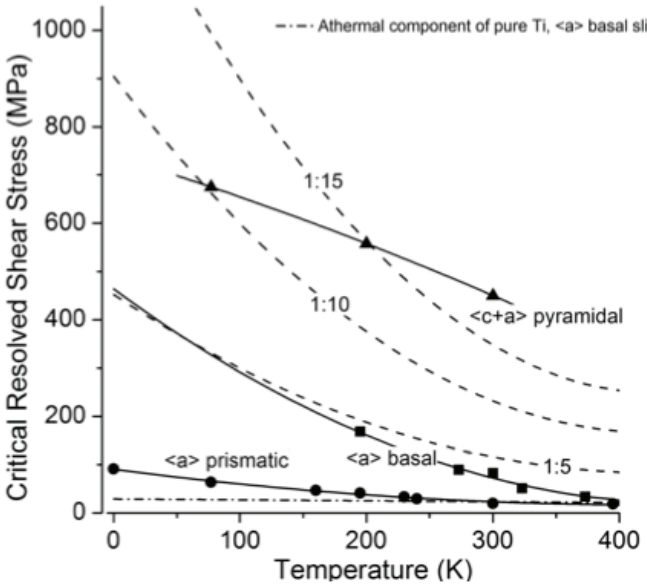

FIGURE 1. Relationship between critical resolved shear stress and temperature for <a> prismatic, <a> basal and <c+a> pyramidal slips in α-Ti. Dash curved lines indicate scales with 5, 10 and 15 times as large as the CRSS of <a> prismatic slip, respectively. Dashed-dotted line indicates the athermal component of <a> basal slip in pure Ti.

TABLE 1. Titanium alloys showing subsurface fatigue crack initiation with transgranular facet in α grain.

Materials	Fatigue Test Condition (loading mode, stress ratio, temperature)	Facet Plane	Inclination of Plane Normal to Principal Stress Axis	Reference
Ti-1Fe-O	normal, R= 0.01, 77 K	(0001)	60°	[3]
Ti-6Al-4V (HIP)	normal, R= 0.1, 300 K	(0001)	40-47°	[7]
(coarse acicular)	normal, R=-1/0, 300 K	$(001)_\beta/(0001)_\alpha$	45-55°	[9]
(Widmastätten)	normal, R=-1/0, 300 K	$(001)_\beta/(0001)_\alpha$	45-55°	[9]
(bi-modal)	normal, R= 0.3, 300 K	(0001)	15-40°	[10]
Ti-6Al-2Sn-1.5Zr-1Mo (Ti-11)	normal, R= 0.1, 300 K	(0001)	<40°	[11]
Ti-8Al-1Mo-1V	normal, R= 0.1, 300 K	(0001)	-	[12]
Ti-6Al-5Zr-Mo-Si	normal, R= 0.1, 300 K	(0001)	<40°	[11]
(IMI685)	normal/dwell, R= 0.1, 300 K	(0001)	0°	[13]
Ti-5.8Al-4Sn-3Zr-Nb-Mo-Si (IMI-834)	dwell, R= 0.1, 300 K	(0001)	-	[13]
Ti-6Al-2Sn-4Zr-2Mo	normal/dwell/static, R= 0, 300 K	(0001)	3-4°/4-12°/19-24°	[14]
	dwell, R= 0.01, 300 K	(01-10)	0°	[15]
Ti-5Al-2.5Sn	normal, R= 0.01, 4 K	(11-21)	60°	[16]

NUMERICAL APPROACH BASED ON FULL CONSTRAINTS MODEL

Application of Taylor Analysis

The full constraints model was adopted to evaluate the CRSSs in the primary slip system of α-titanium at low temperatures.[6] The internal plastic work rate dW and Taylor factor M were also calculated to discuss the effect of the primary slip system on slip behavior and that of the crystal orientation on the stress field. The dW is the increment of work per volume that is the sum of the work of five independent slip systems in a grain with multiple slips:

$$dW = \sum_i \tau_i \left| d\gamma_i \right| \quad (\text{i} = 1, 2\ldots, 5) \tag{1}$$

where τ_i is CRSS from i slip system and $d\gamma_i$ is the slip rate in the i-th slip system. The slip deformation is based on principal of minimum work. Then the dW corresponds the internal plastic work as few as possible. Only one combination is to be chosen. Each time ideal plastic deformation take places, equals the dW as:

$$dW = \tau d\gamma = \sigma_{zz} d\varepsilon_{zz} \tag{2}$$

The M is the newly defined as:

$$\frac{\sigma_{zz}}{\tau} = \frac{\sum_i \left| d\gamma_i \right|}{d\varepsilon_{zz}} = M \tag{3}$$

The M represents the sum of the slip rates in the operating slip systems within a grain per unit strain, and depends on the relationship between the tensile axis (z-axis) and grain orientation.

Predominant slip system was given as {01-10}<11-20>, and effects of secondary slip systems such as {0001}<11-20> and {01-11}<11-23> on the dW were evaluated. No deformation twinning and ε-martensite were considered. Because the CRSSs in the slip systems are different from each other, their ratio was given by the estimated values in Figure 1.

As represented in Figure 2, the rotation angle α ($0^\circ < \alpha < 90^\circ$) along the x-axis in the orthogonal coordinates, xy'z', gives the transform into the orthogonal coordinates, xyz. The angle β ($0^\circ < \beta < 30^\circ$) along z'-axis in the orthogonal coordinates, x'y''z', gives the transform into the xy'z'. In the tension mode, the tensile axis is parallel to z-axis. In the simple shear mode, the shear direction is parallel to x-axis, and z-axis is normal to the shear plane.

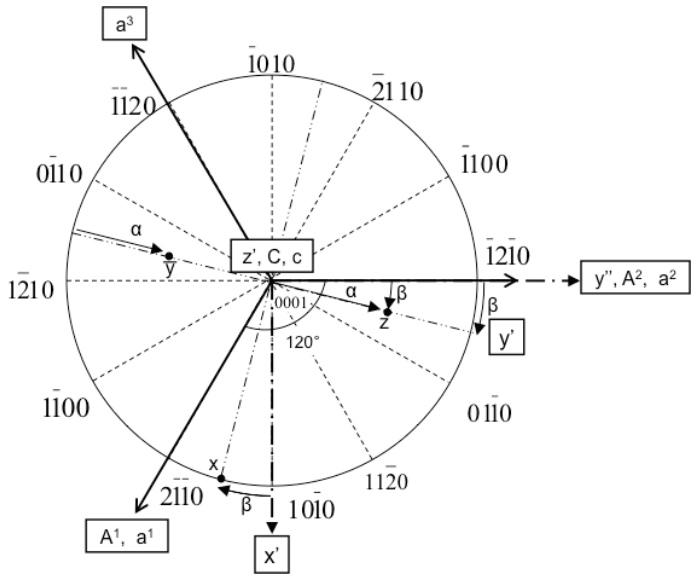

FIGURE 2. Definition of α and β on the standard stereographic projection of (0001) plane with Miller-Bravais index (a^1, a^2, a^3, c), orthogonal coordinates system (x', y", z') and non-orthogonal coordinates system （A^1, A^2, C） in crystal and orthogonal coordinates system (x, y, z) in specimen.

Slip Deformation in Local Yielding Condition

When the tensile axis was around α=40~90 degrees, stress concentration was relaxed by slip deformation because of low dW. Deformation structure mostly covered with {01-10}<11-20>. On the contrary, The dW maximum was appeared at <0001> tensile axis where stress field was developed on the normal to {0001} and hardly relaxed, because the operation of {01-11}<11-23> is suppressed. In order to relax the stress field at {0001}, pyramidal slip must be active as shown in Figure 3. It suggests that the accumulated tensile stress field exists along <0001> and is responsible to initial microcracking and it's opening.

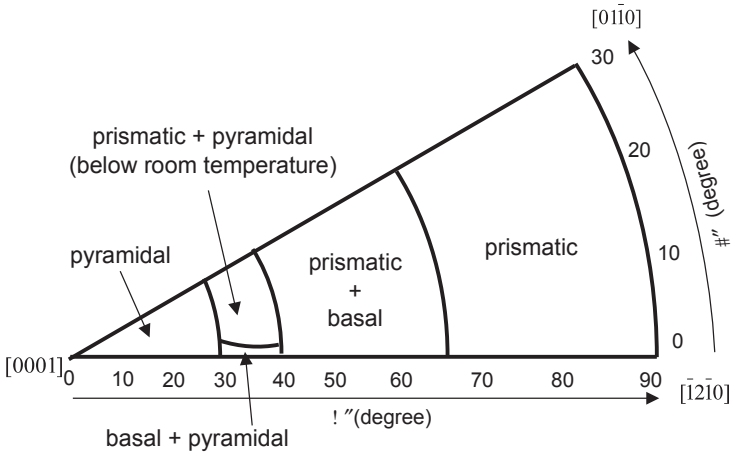

FIGURE 3. Schematic illustration of dominate slip systems for tension in titanium at low temperature.[6]

Slip Deformation in Shear Mode

The heterogeneous deformation in simple shear mode was also analyzed.[17] At almost all of orientations, the plastic relaxation under the simple shear mode was easier than that under the tension mode. The localized basal slip on (0001) under the simple shear mode may assist the growth of microcrack on the plane. Thus the mode II crack

may act on {0001}. The crack-shielding by dislocations causes the fatigue crack closure under mode II and/or mode III. Since the microcrack growth is a consequence of the plastic deformation at the crack tip under the cyclic deformation, it may result from the formation of new surface by slip as well as the formation of surface step. The localized basal slip has a potential to produce the new surface along {0001} under mode II and/or mode III.

The simple shear mode on (01-10) also induced localized slip of {10-10}<1-210> or {0001}<1-210>. The {10-10}<1-210> and {0001}<1-210> were active under near [2-1-10] and [0001] shear direction, respectively. If the microcrack growth is given by the shear of Buerger's vector at the tip, the growth rate of microcrack on {01-10} was higher than that on {0001}.

ORIGIN OF MICROCRACKING AND MICROCRACK GROWTH

Tensile Stress Distribution

Under the local yielding condition, yielding of each grain depends on its crystallographic orientation so that the strain must be installed higher in local yielded grain (soft) than in elastically endured grain (hard). Then the strain incompatibility between the soft grain and the hard one induces a residual stress. The dependence of grain orientation on plastic deformation under tensile stress near yield stress was analyzed by neutron diffraction.[18] In an α-titanium alloy, residual stress was detected as shown in Figure 4. The largest residual tensile stress was normal to (0002), which agreed with the transgranular cracking on {0001}.

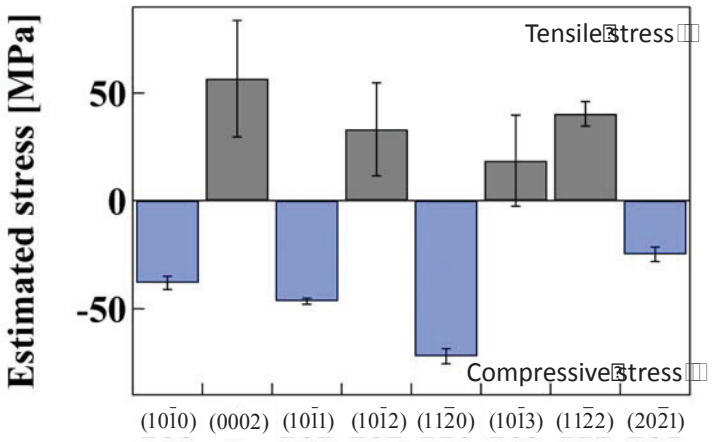

FIGURE 4. Dependence of residual stress distribution on crystal planes under ε=1.0% in the tension.[18]

Crystal Plane of Facets

Although the difference in microstructure influenced the high-cycle fatigue strength of Ti-6Al-V alloy, the subsurface fatigue crack initiation appeared in any kinds of microstructure such as acicular, equiaxed, Widmastätten and bi-modal and its origin was mostly {0001} transgranular cracking as listed in Table 1. The α-colony structure with acicular or Widmastätten α grains exhibited lower fatigue strength in high-cycle regime,[19] because the primary α grains in a colony are believed to be crystallographically aligned and act as a single path for dislocation motion. In that case, the mean slip length becomes several times of primary α grain width. The refinement of α-grain structure and/or the grain distribution with random orientation are effective to lower the maximum stress concentration at a boundary,[4] since shorter slip length leads to substantial improvements in fatigue strength.

Grooved-rolling process was installed to modify the microstructure of Ti-1Fe-O alloy and the effect of grain structure on the subsurface crack initiation was demonstrated.[20] The material showed refined grains with <01-10> fiber texture. However, there was no improvement on the fatigue strength at 10^7 cycles at 77 K. The aggregated {01-10} facets were detected at the subsurface crack initiation site as the dwell fatigue in the reference [15]. It exhibited

low resistance on the microcrack growth on {01-10} to form the fatal crack leading to crack propagation. The reason why {01-10} facets mostly formed in the site will discuss in below.

Microcrack Growth

Dependence of Initiation Site Size on Stress Range

When the microcrack is selected for a main crack, the selection is always competitive and depends on its size and the stress level. The assumption in which the fatigue limit of the material containing pre-existing defect is determined from the relationship between the defect size and threshold stress range can be applicable for the microcrack selection.[1,4] Namely the dependence of subsurface fatigue crack intuition site size on the maximum stress range could be accounted for by the assumption that the microcrack growth was controlled by a critical condition, K_{th}=constant. Thus the microcrack nucleated in an α grain does not always provide a critical main crack size. The microcrack sometimes grows into neighbor α grains, until it finally formed an initiation site for a main fatigue crack. By introducing the ideas of microcrack growth, therefore, a microcrack becomes a fatal crack in a given stress range. An approximate equation to give the maximum stress intensity range ΔK_{Imax} at the subsurface crack tip is represented as follows:

$$\Delta K_{\mathrm{Im}ax} = A\Delta\sigma_{\max}\sqrt{\pi 2a} \tag{4}$$

where A is coefficient, $\Delta\sigma_{max}$ is maximum cyclic stress range and 2a is crack length.

On the basis of the above assumption, Figure 5 shows the dependence of subsurface fatigue crack intuition site size on the maximum stress range of Ti-1Fe-O alloy.[20] The value of $\Delta\sigma_{\max}\sqrt{\pi 2a}$ is in a narrow range so that there is a critical condition, K_{th}=constant, at any stress level where subsurface crack initiation occurs. In the range, there are three groups as indicated by arrows in Figure 5. It may reflect on the numbers of α grains covered by facets as shown in Figure 6. The high cycle fatigue strength, therefore, highly depends on the subsurface crack intuition site size. The aggregated {01-10} facets in the Ti-1Fe-O material may result from lower resistance of microcrack growth. The {01-10} transgranular crack formed in an α grain in the <01-10> aligned regime can easily grow into neighbor α grains, because the crack growth rate on {01-10} facet plane is higher as evaluated in above. It leads to the increase of crack initiation site size.

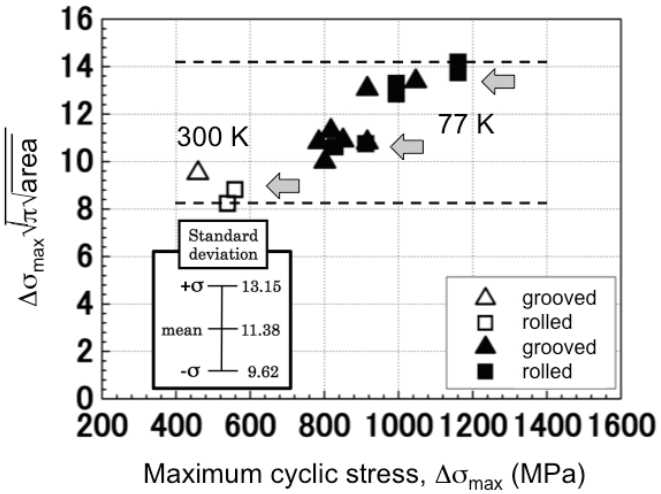

FIGURE 5. Dependence of subsurface fatigue crack intuition site size on the maximum stress range of Ti-1Fe-O alloy.

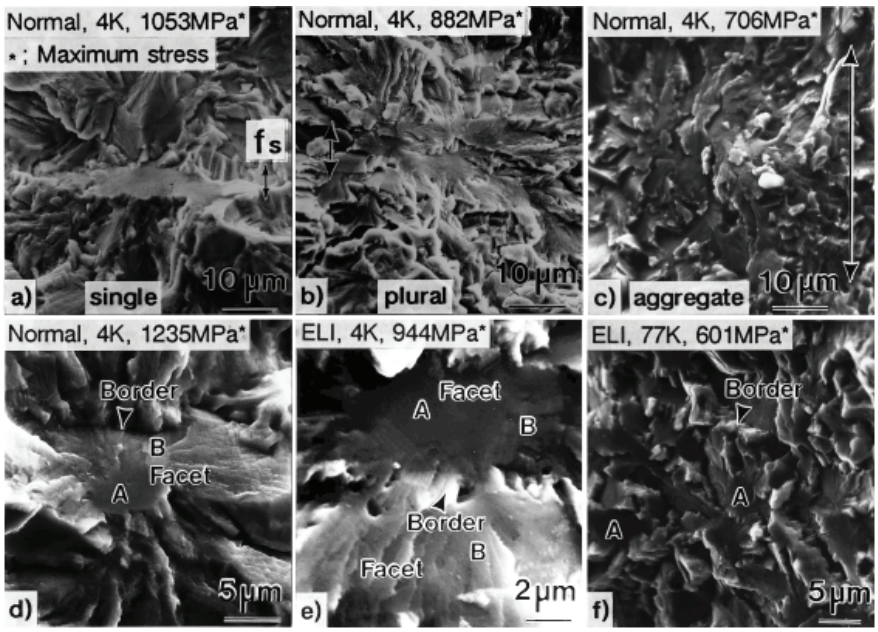

FIGURE 6. SEM micrographs of subsurface crack initiation sites in Ti-6Al-4V alloys.[4]

Microcracking and Microcrack Growth

In the case of a Ti-6Al-4V alloy, detailed observation classifies the subsurface crack initiation site into "Facet" and "Border" parts as shown in Figure 6.[4] The border envelops a facet and has a ductile fracture surface at between facets (Figures 6e)). Furthermore, two regions A and B are found in the facets (Figures 6d and 6e). Region A is a microcracking part of about several μm in diameter. Region A touches a border, and shows fragile cracking surface. Region B gives an appearance of microcrack growth in a radial pattern from region A. Regions A and B on a facet shown in Figure 6d are not always on the same plane against the principal stress axis. Although mostly one region A is found in a site, a few ones are seen in the aggregate type as shown in Figures 6f. One facet may give the region A, and other ones may be formed in the microcrack growth stage.[10,20] In the case of Ti-1Fe-O alloy, microcrack growth may result in {01-10} facets in the site,[20] although its microcracking model has not been clear yet. Both the advanced Stroh model [21] in the dwell fatigue and the localized slip model [3] are not enough to clarify the subsurface microcracking in high-cycle regime.

SUMMARY

Subsurface crack initiation in high-cycle fatigue has been detected as a transgranular cracking on {0001} in α-titanium at and below room temperature. The previous works suggests that strain incompatibility due to heterogeneous deformation may form an opening stress along <0001> and generate crystallographic facet. Nobel analyses on the subsurface crack initiation were summarized and the discussion on the subsurface crack generation was made as follows.

The plastic deformation relaxing the stress field under the tension or simple shear mode in α-titanium alloy at low temperatures was evaluated using the Taylor model. The grain in which the highest rate of plastic work was around tensile stress axis of <0001> was hardly relaxed, since the <c+a> pyramidal slip systems and twinning were inactive at all. Thus the accumulated tensile stress along <0001> may be responsible to initial microcracking on {0001} and the crack opening. The localized basal slip on {0001} under the simple shear mode may assist the growth of microcrack. The simple shear mode on (01-10) also induced localized slip of {10-10}<1-210> or {0001}<1-210>. The growth rate of microcrack on {01-10} was higher than that on {0001}.

The characterization of facet at the subsurface crack initiation site and neutron diffraction analysis under tension mode were also summarized and discussed the role of heterogeneous deformation on the transgranular cracking and its growth in α-titanium. The residual stress distribution was clearly detected and was divided into soft and hard grains. The highest residual stress existed normal to {0001}, which was responsible to transgranular cracking on

{0001}. Those analyses agreed that strain incompatibility due to heterogeneous deformation caused the {0001} microcracking and the microcrack growth formed facet or facets.

REFERENCES

1. O. Umezawa and K. Nagai, *ISIJ International*, **37**, 1170-1179 (1997).
2. O. Umezawa, T. Ogata, T. Yuri, K. Nagai and K. Ishikawa, in *Advances in Cryogenic Engineering Materials*, edited by R.P. Reed, Vol. 40, Plenum Press, NY, 1994, pp. 1231-1238.
3. H. Yokoyama, O. Umezawa, K. Nagai, T. Suzuki and K. Kokubo, *Metall. Mater. Trans. A*, **31A**, 2793-2805 (2000).
4. O. Umezawa, K. Nagai and K. Ishikawa, *Tetsu-to-Hagane*, **75**, 159-166 (1989).
5. M. Hamada and O. Umezawa, *ISIJ International*, **49**, 124-131 (2009).
6. M. Morita and O. Umezawa, *Materials Transactions*, **52**, 1595-1602 (2011).
7. A.L. Pilchak and J.C. Williams, *Inter. J. Fatigue*, **31**, 989-994 (2009).
8. F. Brider, P. Villechaise and J. Mendez, *Acta Mater*., **56**, 3951-3962 (2008).
9. J.A. Ruppen, D. Eylon and A.J. McEvily, *Metall. Trans. A*, **11A**, 1072-1075 (1980).
10. I. Bantounas, D. Dye and T.C. Lindley, *Acta Mater.*, **57**, 3584-3595 (2009).
11. D. L. Davidson and D. Eylon, *Metall. Mater. Trans. A*, **11A**, 837-843 (1980).
12. C.C. Wojcik, K.S. Chan and D.A. Koss, *Acta. Metall*, **36**, 1261-1270 (1988).
13. M.R. Bache, W.J. Evans and H.M. Davies, *J. Mater. Sci.*, **32**, 3435-3442 (1997).
14. V. Sinha, M.J. Mills and J.C. Williams, *Metall. Mater. Trans. A*, **37A**, 2015-2026 (2006).
15. E.E. Sackett, L. Germain and M.R. Bache, *Inter. J. Fatigue*, **29**, 2015-2021 (2007).
16. Y. Ono, M. Demura, T. Yuri, T. Ogata, S. Matsuoka and S. Hori, *Trans. Japan Soc. Mech. Eng. Ser. A*, **74**, 329-334 (2008).
17. M. Morita and O. Umezawa, in *Proceedings of the 12th World Conference on Titanium (Ti-2011),* edited by L. Zhou, H. Chang, Y. Yu, D. Xu, Science Press Beijing, 2012, Vol. 2, pp. 1100-1103.
18. M. Morita, S. Morooka and O. Umezawa, "General Paper Selections" in *Supplemental Proceedings*, TMS, Warrendale, 2011, Vol. 3, pp. 427-431.
19. O. Umezawa, K. Nagai, H. Yokoyama and T. Suzuki, in *High Cycle Fatigue of Structural Materials*, edited by W.O. Soboyejo, T.S. Srivatsan, TMS, Warrendale, 1997, pp. 287-298.
20. T. Yuasa, O. Umezawa and Y. Ono, in *CAMP-ISIJ*, Vol. 24, 2011, pp. 1058.
21. M.R. Bache, *Inter. J. Fatigue*, **25**, 1079-1087 (2003).